Journal of the Indian Society of Remote Sensing
https://doi.org/10.1007/s12524-026-02616-6

RESEARCH ARTICLE

Identification of Potential Fishing Zone (PFZ) Hotspot Using Thermal Front and Ecosystem Productivity Indicators Along the Southwest Coast of India

Harisha Rathod[1] · P. C. Mohanty[1] · J. Nithya[1] · J. Karthi[1] · Dhanya M. Lal[1] · Alakes Samanta[1] · Sanjiba Kumar Baliarsingh[1] · Sudheer Josheph[1] · T. M. Balakrishnan Nair[1]

Received: 24 September 2025 / Accepted: 18 October 2026
© Indian Society of Remote Sensing 2026

Abstract
Thermal fronts (TF) are critical in regulating physical-biological interactions and fish aggregations along the southwest (SW) coast of India. This study examines the spatial and temporal variability of Thermal Front Frequency (TFF) and TF linkage with ocean productivity during 2020–2023. TFF was higher in the northern sector, 15–18°N and declined as the measurements were taken down south, that is, 8–10°N, with a different latitudinal gradient clearly distinguished. Seasonally, the highest occurrence of TFF is in winter, and it starts decreasing during the pre-monsoon season. The monsoon season is marked by intense clouding and a large amount of freshwater entering the seawater, which is not favourable for the formation of TF, whereas the post-monsoon season marks an increase in TFF. Positive TF-Net Primary Productivity (NPP) relationships were observed in regions where elevated TFF were noted, which demonstrated the existence of fronts in nutrient convergence and retention. The relationship between TFD and fish catch happened after two days ($r=0.40$) while chlorophyll-a had its link with thermal front after about one day ($\tau=0.357$ $p<0.05$). Satellite-based TFD, when combined with chlorophyll-a wind-driven measures and other important oceanographic and fisheries factors could serve as an extra tool for describing possible fishing areas and helping with fisheries prediction and ecosystem-focused management, along the southwest coast of India.

Keywords Thermal front frequency · PFZ Hotspot · Sea-leve anomaly · Upwelling · NPP · Remote sensing etc

Introduction

Marine fisheries are an important part of the global economy and play an essential role in providing food and nutritional security. Nevertheless, an industrialization of the fishing fleet and overfishing have put tremendous pressure on marine fisheries (Pauly & Palomares, 2005). The Blue Economy provides a comprehensive lens of sustainable development based on the ocean's use by considering at the same time economic growth and environmental protection based on assessing the economic potential of marine resources. Monitoring fisheries are particularly important in coastal nations where marine ecosystems provide the foundation for livelihoods, cultural heritage and economic security. Marine capture fisheries currently produce around 79.7 million tonnes globally (FAO, 2024) provide nutritious protein to more than 3 billion people and support the livelihoods of more than 200 million people particularly in coastal developing countries.

Capture fisheries are intricately linked to the UN Sustainable Development Goals (SDG) SDG 1 (No Poverty), SDG 2 (Zero Hunger), SDG 8 (Decent Work and Economic Growth) and SDG 14 (Life Below Water). Sustainable use of marine fish stocks alleviates hunger and poverty and can also contribute to a healthy ecosystem in the long term while enhancing economic growth (FAO, 2020). Sustainability is a balancing act between exploitation and conservation, a

✉ P. C. Mohanty
prakash.marine@gmail.com

T. M. Balakrishnan Nair
prakash.marine@gmail.com

[1] Ministry of Earth Sciences, Indian National Centre for Ocean Information Services (INCOIS), Govt. of India, Hyderabad 500090, India

Published online: 15 November 2026

process that is enabling through advanced tools such as satellite derived ocean data, habitat modelling and predictive fisheries forecasting. The sustainable management of fisheries has begun using PFZ (Potential Fishing Zone) advisories from indicators such as Sea Surface Temperature (SST) fronts and chlorophyll-a (chl-a) concentrations.

In 2022, world fisheries and aquaculture production totalled 223.2 million tonnes (FAO, 2024). Generally, fishery yields are predominantly determined by marine productivity, so fishery catches tend to be on the higher side in coastal regions that are subject to upwellings and frontal zones. Ocean fronts or areas where water masses with differing temperature, salinity or nutrient levels collide are especially important as they enhance vertical mixing allow nutrients to build up in the surface water and trigger phytoplankton blooms that stimulate higher trophic levels.

From a global perspective, there is a clear body of literature highlighting the ecological and fisheries significance of ocean fronts. For example, the transition zone chlorophyll front (TZCF) in the North Pacific provides a critical foraging habitat for pelagic species such as skipjack tuna and Pacific saury (Polovina et al., 2001; Mugo et al., 2014; Tseng et al., 2014). In coastal upwelling environments such as the California current and Canary current, the temporal and spatial distribution of fish species is largely driven by oceanic fronts and upwelling, which in turn attract larger predatory species including turtles and seabirds (Reese et al., 2011; Scales et al., 2015). Similarly, in Mauritanian waters, pelagic species associated with upwelling fronts, such as mackerel and sardinella are abundant (Ebango Ngando et al., 2020). In addition, fish and other predator aggregations at higher latitudes (e.g., Subtropical Front, Subantarctic Front & Polar Front) further illustrate the ecological engine role of ocean fronts (Bost et al., 2009; Cox et al., 2016; Miller et al., 2015). Collectively, these examples highlight ocean fronts as ecological engines that concentrate biodiversity and provide meaningful foraging opportunities across latitudes.

Remote sensing has transformed the detection and monitoring of these features. Pioneering initiatives, such as Belkin & Cornillon's (2009) global frontal atlas, showed not only are there seasonal changes but demonstrated the ecological role of these features. Studies published in recent years are indicating opposing trends; frontal activity in the subtropical gyres is declining and frontal activity and productivity during climate change in higher latitudes is increasing (Yang et al., 2023).

In the Indian Ocean, Thermal Fronts (TF) have been recognized as both persistent and ecologically important features to regulate circulation, nutrient transport and fish distribution. The West India Shelf-Slope Front (WISSF), West India Mid-Shelf Front (WIMSF) and the Gulf of Mannar Front (GMF) are some of the examples of TF that have seasonal cycles (Sarkar et al., 2019). Shelf associated fronts tend to be more productive because of nutrients supplied through upwelling, while open ocean fronts have productivity sustained by microbes (Sarma et al., 2018). In the Northeast Arabian Sea, 45–75% of TF reoccur every year indicating their persistence and reliability as an indicator of productive fishing areas (Mohanty et al., 2017).

Recent studies have highlighted the growing importance of satellite derived TF in understanding physical-biological coupling and fisheries productivity in the northern Indian Ocean. For instance, Swapna et al. (2023) and Chakraborty et al. (2019) demonstrated that frontal activity along the Indian coast exhibits strong seasonal modulation with enhanced persistence during winter and post-monsoon periods due to intensified thermal gradients and reduced cloud cover.

Along the Southwest (SW) coast of India, the narrow continental shelf and pronounced shelf break (~50–200 m isobaths) promote the interaction between coastal and offshore water masses. These bathymetric features intensify wind driven upwelling during the southwest monsoon and influence post-monsoon destratification, thereby strengthening cross shelf temperature gradients that favour TF development (Shankar et al., 2005).

New developments in algorithms, such as the Cayula Cornillon edge detection technique have made possible accurate mapping of TF from satellite SST observations. Studies using MODIS SST and blended (G1SST) datasets with the optimal thermal gradients of around 0.07–0.075 °C/km, reported strong seasonal variability of fronts along the Indian coast from 2014 to 2020 (Swapna et al., 2023). These studies showed both transient and persistent patterns, highlighting fronts as being critical to PFZ.

The importance of the PFZ advisories is most evident along India's southwestern coast (Kerala, Karnataka, Goa & Maharashtra) which accounts for a substantial part of the country's marine landings (3.53 million tonnes in 2022, CMFRI 2023). PFZ advisories are operational and delivered daily to fishers by ESSO-INCOIS using SST and chl-a data collected from NOAA-AVHRR, MODIS-Aqua and Oceansat-2. PFZ advisories help reduce search time and fuel consumption during fishing operations.

The benefits of PFZ advisories have been supported by field validation. For instance, in Kerala during 2022-23, the landings of fishers showed a clear increase on PFZ days with analysis of trophic guilds revealing that landings were dominated by planktivorous and followed by carnivores (Lal et al., 2025). Overall, this demonstrates how PFZ advisories translate oceanographic information into socio-economic benefit.

Frontal systems also provide distinct ecological functions. For example, the tropical southeast Indian ocean provides the only known spawning habitat for southern bluefin tuna, as weak (but consistent) SST and chl-a fronts help support plankton high habitats that are important for larval growth (Nieblas et al., 2014). Further up the coast of the Indian ocean, Stronger frontal activity during winter is driven by enhanced surface cooling, sharper horizontal SST gradients and stable atmospheric conditions associated with the northeast monsoon, along with intensified coastal current interactions and reduced cloud cover, which together promote the formation and persistence of seasonal PFZ (Chakraborty et al., 2019).

The persistence, strength and ecological roles of frontal systems further demonstrate their importance to fisheries and ecosystem productivity.

TF in the eastern Arabian sea arise from strong horizontal temperature gradients associated with monsoon-driven circulation, coastal upwelling, wind-induced mixing and mesoscale eddies along the SW coast of India. (Schott & McCreary Jr, 2001; Shetye et al., 1990; & Bruce et al., 1994). These processes exhibit pronounced seasonal variability under the influence of the southwest and northeast monsoons, strongly modulating upper ocean structure and biological productivity (Schott & McCreary Jr, 2001; Wyrtki, 1973; Shankar et al., 2002).

Overall, the Indian Ocean fronts operate as dynamic ecological boundaries that link oceanographic processes to fisheries production. The advancement in research from early observations to present day operational fisheries advisories shows how important they are for both scientific and management purposes.

In light of the above context, the present study uses daily 1.1 km Advanced Very High-Resolution Radiometer (AVHRR) SST (NOAA-18) data to delineate TF that serve as proxies for productive fishing zones along the SW coast of India. Gradient threshold of 0.3 °C per pixel was used to find biologically important fronts. The choice followed the sensitivity analysis of Mohanty et al. (2017). Mohanty et al. Argued that thermal gradient threshold offers a balance: it keeps enough front details while focusing on stronger thermal gradients that match high Chl-a levels. With advances we aim to (i) describe how thermal frontal frequencies (TFFs) vary each month and each season; (ii) locate frontal hotspots and investigate what physical forces might create them; (iii) study the timing of thermal-front density (TFD) chlorophyll-a concentration, fish catch, sea-level anomaly (SLA) and geostrophic current (GC) to understand who leads and who follows; and (iv) analyse how thermal fronts relate to other physical and biological factors along the SW coast of India namely photosynthetically active radiation (PAR) net primary production (NPP) stratification (STF) and Ekman pumping (EKP). The study period is from January 2020 to December 2023. This four-year span gives an overlap, between ocean data from satellite sensors and commercial fish landings from Captain Fresh. This overlap lets us continuously observe how SST-derived thermal fronts, Chl-and other variables change across years, seasons and months and how these changes connect to fish landings.

By linking TF dynamics with environmental indicators and fishery outcomes, this study contributes to a better understanding of how ocean fronts support sustainable fisheries and enhances the operational value of PFZ advisories in line with the Blue Economy vision.

Materials and Methods

Study area

The study location is located in the SW coast of India (Fig. 1) and exhibits complex ocean atmosphere coupling. The Indian Summer Monsoon (ISM, June-September) takes the lead among the significant forcing mechanisms by inducing mixing and upwelling and therefore increasing primary productivity along the west coast (Sarupria & Bhargava, 1993; Madhupratap et al., 2001; Habeebrehman et al., 2008). This productivity serves an important role to provide for rich fisheries that are important for the area as a marine resource. Field studies further validate that the PFZ advisories were valuable and improved Catch per unit effort (CPUE) and profits for the longline fishery along the Kerala coast (Pillai & Nair, 2010).

The extent of present study area constraint 69 to 78E Longitude and 7 to 18 N Latitude, consisting of southern part of Maharashtra (MH), Goa, Karnataka (KA), Kerala (KL) & and the adjoining Lakshadweep Sea.

Data and Methodology

SST data were obtained from the AVHRR onboard National Oceanic and Atmospheric Administration (NOAA-18) satellites for the period 2020–2023. SST products with a spatial resolution of 1.1 × 1.1 km were used for TF extraction.

TF were detected using the open-source Marine Geospatial Ecology Tools (MGET v0.8a79, Python 2.6), developed by the Marine Geospatial Ecology Lab, Duke University. The tool implements the Cayula and Cornillon (1992) single-image edge detection algorithm within the GeoEco Python package, which identifies frontal boundaries based on SST gradient and histogram segmentation techniques. Monthly composites of TF occurrence were generated from daily detections for subsequent climatological and statistical analyses.

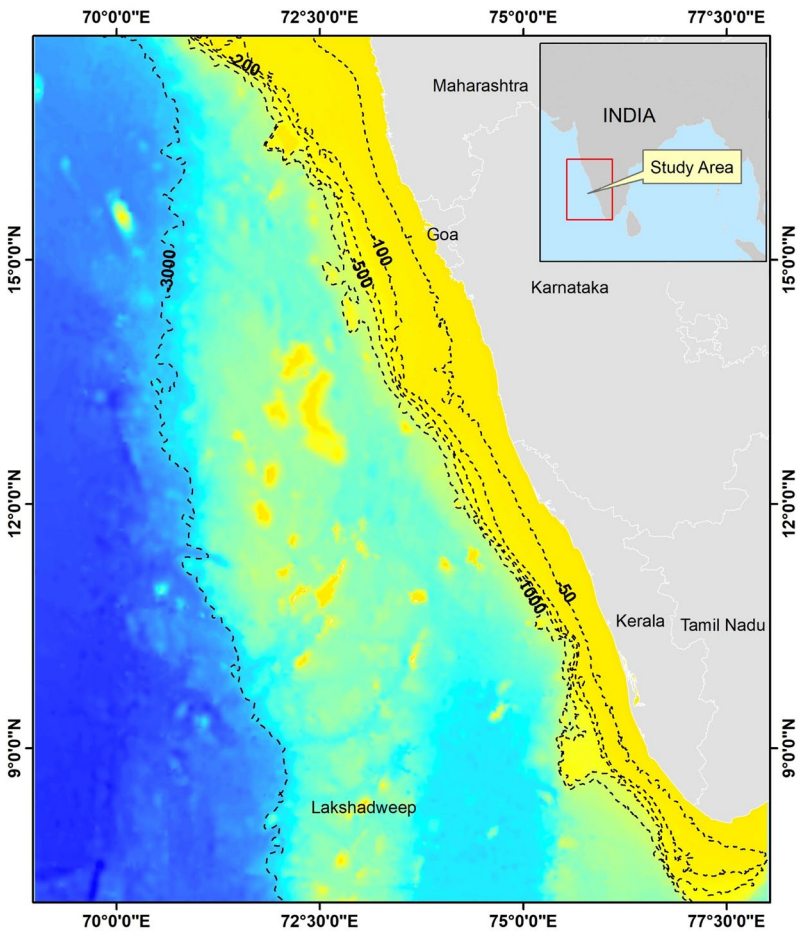


Fig. 1 Map of the study region along the SW coast of India showing bathymetric contours and key coastal states

Visible and infrared image/Radiometer suite/Suomi-NPP NOAA20 (VIIRS) level-3 daily global Chlorophyll concentration (mg/m^3), DINEOF Gap filled data processed by NOAA NESDIS Coast watch are downloaded from Jan to May 2023 for establish the lead-lag relation between TFD and daily gap filled chl-a concentration and it presented in results section. The fishery data included 26 sampling points that were marked with locations. These points were gathered between January and May of 2023. The fishing activities used a variety of fishing tools. These tools included Purse seines, Trawlers, Hook-and-line Gill nets, Ring nets and Bottom trawling. The data therefore comes from a type of commercial fishing. This type of fishing targets kinds of fish and uses various ways to catch them. Information about the boats, such as the size of the boats and the power of their engines and details about how long they fished and how much effort they put into using each type of gear was not always available. Because of this the catch data was used as it was reported by the fishermen. It was not adjusted to be a measure of catch per unit effort. The differences between the boats how long they fished, how efficient the gears. The types of fish they targeted were all seen as possible reasons for changes, in how the catches related to the environment.

The Cayula and Cornillon (1992) algorithm identifies fronts by detecting boundaries between two statistically distinct pixel groups showing a bimodal temperature distribution within an image window. For SST, these boundaries represent interfaces between different water masses. The strength of a front depends on the gradient, i.e., the average temperature difference between the two modes, with larger differences indicating stronger fronts.

In this study, pixels with SST gradients above a 0.3 °C per pixel threshold (Mohanty et al., 2017) were classified as fronts (value = 1), while others were non-fronts (value = 0). A 32 × 32 pixel moving filter kernel was applied to reduce noise and sharpen frontal boundaries. Further, a semi-automated ArcGIS tool was developed to refine and extract TF as line features, enabling subsequent analysis and potential routine use for identifying productive fishing grounds.

To reduce high frequency noise in the SST imagery, a median filtering technique was applied prior to analysis. The SST data were processed using a 3 × 3 moving window, wherein the value of each central pixel was replaced by the median of the surrounding pixel values within the window. This non-linear filtering approach effectively suppresses impulsive noise while preserving important spatial features

such as thermal gradients and frontal boundaries, thereby improving the reliability of subsequent frontal detection analysis (Jishad & Agarwal, 2022).

Daily SST derived fronts were aggregated to generate monthly and seasonal climatologies (winter: Jan-Feb; pre-monsoon: Mar-May; southwest monsoon: Jun-Sep; post-monsoon: Oct-Dec) for 2020–2023. TFF (%) maps were then constructed to illustrate the spatiotemporal variability of ocean surface dynamics along the SW coast of India. The TFF was calculated using the Eq. (1).

$$TFF(\%) = \frac{\sum of\ number\ of\ days\ with\ front\ detected\ during\ climatological\ period}{Total\ number\ of\ valid\ observations\ days} \times 100 \quad (1)$$

TFF indicates how often a front occurs at a specific location, reflecting processes such as coastal upwelling and nutrient enrichment. Frequency maps (Fig. 2) display warmer colours where fronts occur more frequently, highlighting productive regions. TFD (%) was calculated to assess relationships with chl-a concentration (mg/m³) and georeferenced fish catch data (tonnes). TFD values were derived from 1.1 km AVHRR SST data using Eq. (2). The 0.5° × 0.5° spatial window around georeferenced sampling points along the SW coast of India was applied. These TFD percentages were subsequently correlated with chl-a levels and fish catch data for ecosystem fisheries linkage analysis.

$$TFD(\%) = \frac{Number\ of\ pixels\ identified\ as\ TFs\ with \in 50km\ buffer}{Total\ number\ of\ valid\ pixels \in the\ selected\ buffer\ 50km} \times 100 \quad (2)$$

Correlation analysis was conducted between the dates of fish catch and lag/lead days of TFD. Moreover, the relationship between TFD and lag/lead days of chl-a concentration was explored to understand the physical-biological interactions in the study area.

SLA was obtained from the Copernicus Marine Service ocean gridded Level 4 dataset with a spatial resolution of 0.125°. GC data were also taken from the Copernicus Marine Service Multi Observation Global Ocean Geostrophic product, which has the same spatial resolution of 0.125°. Chlorophyll-a concentration SLA and GC were then linked to TFD to assess how they relate. This was done using Kendall's rank correlation coefficient (τ). Sen's slope estimator. Kendall's τ is a non-parametric method that measures how strong and in what direction two variables are related based on how their values rank relative, to each other. Sen's slope gives an estimate of how fast a trend is changing and in which direction it is going.

PAR data were obtained from the NASA ocean colour MODIS sensor at 9 km spatial resolution. NPP was estimated from MODIS-derived ocean color products using the Vertically Generalized Production Model (VGPM). NPP was calculated using the VGPM approach, which integrates chl-a concentration, PAR and SST to estimate vertically integrated primary productivity. Wind data required for EKP estimation were acquired from the European Organisation

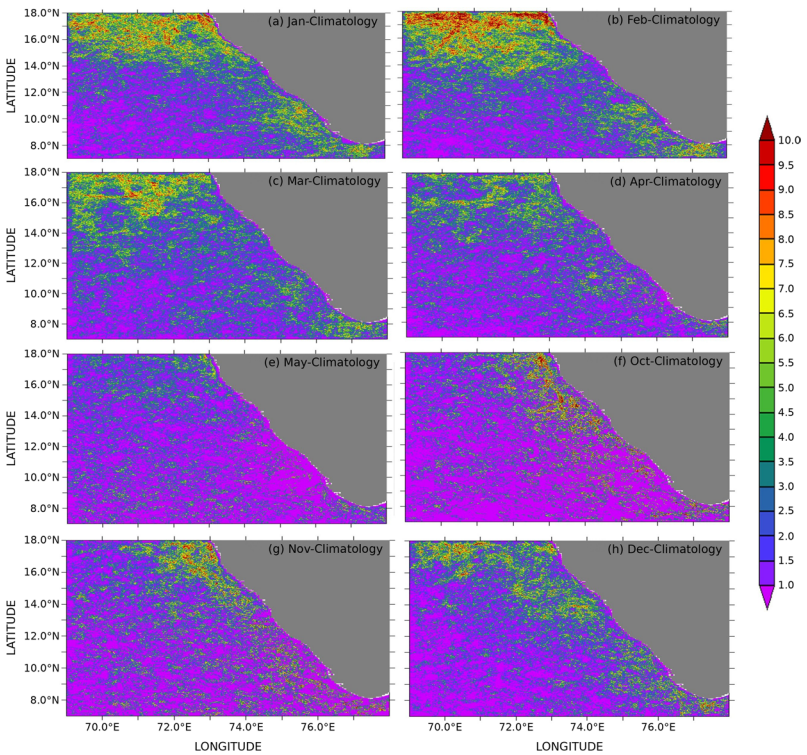


Fig. 2 Monthly climatology of TF along the SW coast of India during 2020–2023, **a**: January, **b**: February, **c**: March, **d**: April, **e**: May, **f**: October, **g**: November and **h**: December showing the spatial distribution of monthly TFF (%)

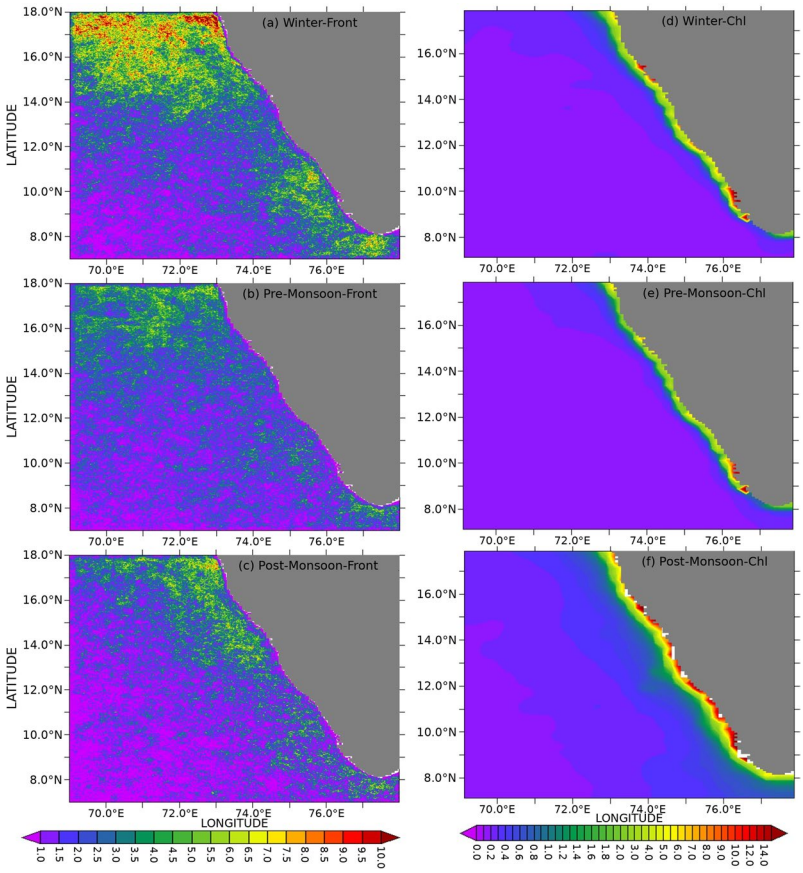


Fig. 3 Seasonal variability on percentage of TFF in **a** Winter-front, **b** Pre-monsoon-front, **c** Post-monsoon-front and Seasonal dynamic of chlorophyll (mg/m^3) concentration **d** Winter-Chl, **e** Pre-monsoon-Chl and **f** Post-monsoon-Chl along the SW coast of India (2020–2023)

for the Exploitation of Meteorological Satellites Advanced Scatterometer (ASCAT) at 25 km spatial resolution.

EKP velocity was computed (Gill, 1982) from ASCAT wind stress fields using the curl of wind stress using the Eq. (3).

$$W_E = \frac{1}{\rho f}(\nabla \times \tau) \tag{3}$$

where, W_E (say EKP) is the Ekman Pumping velocity, ρ is seawater density, f is the Coriolis parameter and τ is Surface wind stress vector (τ_x, τ_y).

Water column STF was derived from temperature and salinity profiles obtained from the National Oceanic and Atmospheric Administration Global Ocean Data Assimilation System (GODAS) using Eq. (4). STF intensity was quantified from GODAS temperature and salinity profiles by calculating density gradients within the upper water column.

$$water\ stability\ Index = \frac{\nabla \rho}{\nabla z} \tag{4}$$

Where is seawater density calculated from water column temperature and salinity as a function of depth (z).

Spatial distribution maps of TF with PAR, NPP, STF and EKP were generated using corresponding climatological data. These maps were used to assess spatial patterns, identify regions of enhanced productivity and examine the linkage between TF and potential fishery hotspot zones.

Results and Discussion

Monthly Variability of TFF Along the SW Coast of India

Higher frontal activity (Fig. 2a) was more prominent along the southern coast of MH (9.0–9.5%). The increased frontal activity could be a result of greater surface mixing that enhance horizontal contrast in SST and thereby frontal formation for this area. Mid-southern regions of MH and offshore regions also show frontal activities with comparatively lower frequencies (5.5–7.5%), suggestive of a decrease in such activities with increasing distance from the coastal areas. Moderate frontal activities (2.5–5.5%) prevailed along the coasts of Goa, northern KA and southern KL, possibly a result of season-specific winds and associated thermally driven coastal circulations. On the other hand, very low frontal activities (1.0–2.5%) prevailed along

offshore KA, KL and Lakshadweep seas that might depict greater similarity and less thermodynamic forcing for these regions.

During the following period, the TFF enhanced even stronger over mid-MH (8.5–10.0%) (Fig. 2b), suggesting an increase in frontal development over this area. This is believed to be linked to enhanced upwelling along the coast. Moderate frequencies of TF were noticed along the coast of southern MH (6.0–7.5%) and similar frequencies of 4.5–6.0% were noticed over northern and southern parts of KL, which may relate to winds and resultant circulation. On the other hand, lower frequencies of frontal development were noticed along the coast of KA and Goa, as well as around Lakshadweep (1.5–3.0%), which is consistent with weaker upwelling signals.

There are dynamic frontal conditions that continued to exist offshore mid-MH (8.0–9.5%) during the period (Fig. 2c), probably because of the weaker water stability led to intense mixing process with residual winter-induced mixing. The Goa, KA, KL and Lakshadweep coasts continued to have moderate TF activity (5.0–6.5%), because of the combined effects of reduced seasonal forcing and local circulation. In the offshore, the frequencies of TF are relatively lower (2.5–4.5%) in agreement with reduced dynamical forcing coupled with similar thermal conditions.

A transition period marked by the weakening of surface thermal gradients is identifiable in Fig. 2d, probably supporting increasing pre-monsoonal STF and a decrease in wind-induced mixing. Thus, frontal activity reduced over the mid-MH coast (6.0–7.5%) and the south (4.0–6.5%) contributed by reduced oceanographic activity and decreased horizontal SST gradients. The decreased SST variability in the transition period implies reduced nutrient supply to the surface layer, possibly limiting its bio productivity.

As seen in Fig. 2e, there was a continuous thinning of frontal features over the study area and only the mid of MH coast maintained a low persistence of TF (5.0–6.5%). Comparative analysis showed that frontal occurrence was very low (1.5–3.5%) at Goa, KA, KL and also at Lakshadweep, emphasizing a decrease in surface thermal features. The decrease in frontal occurrence at a later stage of pre-monsoon seasoning would be attributed to strengthened STF with an expansion of mixed layers and downgrading of upwelling strength that reduces surface temperature contrasts.

During the SW monsoon period (June-September), the occurrence of TF was minimal, likely due to intensified vertical mixing, substantial freshwater influx and persistent cloud cover which collectively reduced surface thermal gradients and weakened frontal signatures. However, owing to extensive cloud cover limiting reliable SST retrieval, the southwest monsoon season is not depicted in this analysis and was therefore excluded from the present study.

During the post-monsoon transition phase (Fig. 2f), renewed oceanographic activity was observed along the mid-MH coast, where TF frequencies increased to 7.5–8.5%, likely driven by the re-intensification of winds that sustain coastal current circulation. Moderate TFF (5.0–6.5%) extended along the Goa, KA and KL coasts, while the Lakshadweep region exhibited comparatively lower but discernible frontal activity (4.0–5.5%), indicating the initial revival of frontal formation across the study region. During the subsequent post-monsoonal stage (Fig. 2g), frontal associated productivity intensified further along the MH coast (8.0–9.5%) due to enhanced surface cooling, nutrient enrichment and the development of convergence zones that strengthened lateral thermal gradients. Moderate frontal activity persisted along the Goa and KA coasts (5.0–6.5%), whereas lower frequencies were recorded along KL and Lakshadweep (2.5–3.5%), consistent with reduced forcing and lower surface variability. In Fig. 2h, frontal activity remained elevated along the mid-coastal zones of MH (7.0–9.0%), sustained by dynamic circulation and reinforced horizontal thermal gradients under evolving winter conditions. Strong TFF were also observed along the coasts of Goa and northern KA (6.0–8.0%), while slightly lower values characterized the KL coast (4.0–6.0%), reflecting latitudinal variations in wintertime forcing. In contrast, the Lakshadweep region showed minimal frontal activity (3.0–4.0%), consistent with more stable offshore thermal conditions.

Frontal detection is based exclusively on satellite derived SST, which represents only surface thermal structure. Subsurface fronts and density driven features may not be captured, particularly during monsoon period or freshwater influence.

TF are well established proxies for increased productivity and have been commonly used for PFZ mapping (Castillo et al., 1996; Solanki et al., 1998, 2001a, b, 2003, 2005, 2008; Nayak et al., 2003; Dwivedi et al., 2005; Das et al., 2010; Pillai & Nair, 2010; Deshpande et al., 2011; Nammalwar et al., 2013; Subramanian et al., 2014). The monthly analysis showed consistently higher TFF along northern part compared to the southern part of the region which corresponds to areas of greater biological productivity. This provides further evidence that TF are reliable PFZ indicators (Solanki et al., 2005; Pillai & Nair, 2010).

The observed seasonality emphasizes the influence of wind driven circulation and STF on regional productivity. Frequent winter and post-monsoon fronts correspond to stronger nutrient supply and biological enrichment, while pre-monsoonal weakening and monsoonal suppression highlight the dynamic coupling between physical processes and ecosystem responses.

Seasonal Variation of TFF in Relation to Chlorophyll Concentration Along the Southwest Coast of India

A clear seasonal variation of TF activity was evident along the SW coast of India. During winter (Figure. 3a), the middle and offshore regions of the MH coast exhibited the highest frontal frequencies (9.5–10.0%), indicating the presence of strong surface thermal gradients, whereas the southern coastal and shelf-break regions showed comparatively moderate frontal activity (6.5–7.5%). These gradients are primarily driven by northeast monsoon induced wind forcing, which modulates coastal circulation, promotes the southward flowing West India Coastal Current and enhances the localized upwelling along the shelf and shelf-break regions (Chakraborty et al., 2019). The pre-monsoon period (Figure. 3b) showed a progressive weakening of frontal activity with the intensification of STF and decline in wind driven mixing, leading to weak SST variability and reduced frontal frequency. This is followed by a gradual recovery of TF activity during the post-monsoon season (Figure. 3c), due to partial recovery of wind driven circulation, erosion of STF and renewed mesoscale processes. The southwest monsoon season is not depicted in this analysis due to persistent cloud cover and therefore it was not considered in the present study.

The left panels (a-c) illustrate the seasonal variability percentage of TFF, while the right panels (d-f) depict the corresponding seasonal distribution of chlorophyll-a concentration along the SW coast of India. A clear spatial coherence is observed between frontal activity and chlorophyll enrichment across all seasons. During winter (a & d), elevated TFF is concentrated along the northern and nearshore regions (8.5–10.5%), which closely aligns with higher chlorophyll concentrations along the coastal belt. While southern KL coast also showing high chlorophyll (9–10.5 mg/m^3). This suggests that persistent TF enhance vertical mixing and nutrient supply promoting phytoplankton growth.

In the pre-monsoon season (b & e), frontal activity weakens and becomes patchier compared to winter and chlorophyll concentrations show a relatively narrower high-value band confined to the immediate coastal zone. The reduced frontal intensity likely reflects increased stratification, limiting offshore nutrient transport and thereby constraining chlorophyll distribution.

During the post-monsoon period (c & f), TFF intensifies again along the coastal and mid-shelf regions (7.5–10 mg/m^3), coinciding with a broader and stronger chlorophyll signal extending offshore. This pattern indicates renewed frontal formation associated with monsoon-driven hydrographic adjustments, facilitating nutrient entrainment and enhanced primary productivity.

In the spatial concordance between TFF (left panels) and chlorophyll distribution (right panels) demonstrates that TF act as ecological hotspots, regulating phytoplankton dynamics through frontal-induced nutrient enrichment processes.

Overall, this seasonal cycle highlights the dominant role of physical forcing in regulating TF formation, persistence and associated productivity patterns across the region.

Spatial Distribution of Mean & SD of TFF

The spatial distribution of the mean and SD of TFF from January 2020 to October 2023 (excluding the monsoon months of June-September), shown in Fig. 4, reveals marked regional variability across the SW coast of India. Excluding the monsoon period reduces cloud-related data gaps in AVHRR (~1 km) SST imagery, ensuring that the derived frontal statistics reflect true oceanographic variability rather than satellite observational bias.

The average TFF map (Fig. 4a) shows prominently higher frontal occurrence in the northern sector (approximately 15–18°N), particularly offshore from the Maharashtra coast. Frequencies count gradually goes down in the southern sectors towards 8–10°N. The higher frontal occurrence in the northern sector was explained by weaker STF (Fig. 8c) which led to dynamical mixing which induced availability of nutrients thorough upwelling processes. These high-mean areas correspond to regions where positive correlations between TF and NPP (Fig. 8b) are observed, indicating that persistent fronts magnify biological productivity via convergences and retention processes on nutrients. Frontal zones inherently enhance the horizontal gradients to ensure vertical supply of nutrients when supported by wind-driven upwelling. In contrast, the southern sector has relatively lower average TFF, indicating a lesser number of persistent frontal structures, possibly linked to minimal upwelling, strong STF (Fig. 8c and d) and the dominance of homogeneous water masses away from the peak upwelling zone.

The SD map (Fig. 4b) complements to this interpretation by revealing spatial variability of frontal occurrence. It is complemented by both interpretations with higher SD found in the northern and central offshore regions coinciding with regions of high mean TFF. This means that there is not only a lot of frontal activity in these regions but also a lot of dynamic variability in that activity. Episodic wind forcing and intermittent upwelling pulses probably account for such variability. In comparison, SD values are comparatively less in the southernmost sector, indicating the presence of stable frontal conditions there with fewer temporal variations. The northern zone shows some degree of seasonal and mesoscale modulation of frontal intensity based especially on the combined high mean and the high SD. The uniformity in PAR-TF (Fig. 8a) offshore relationship indicates light is

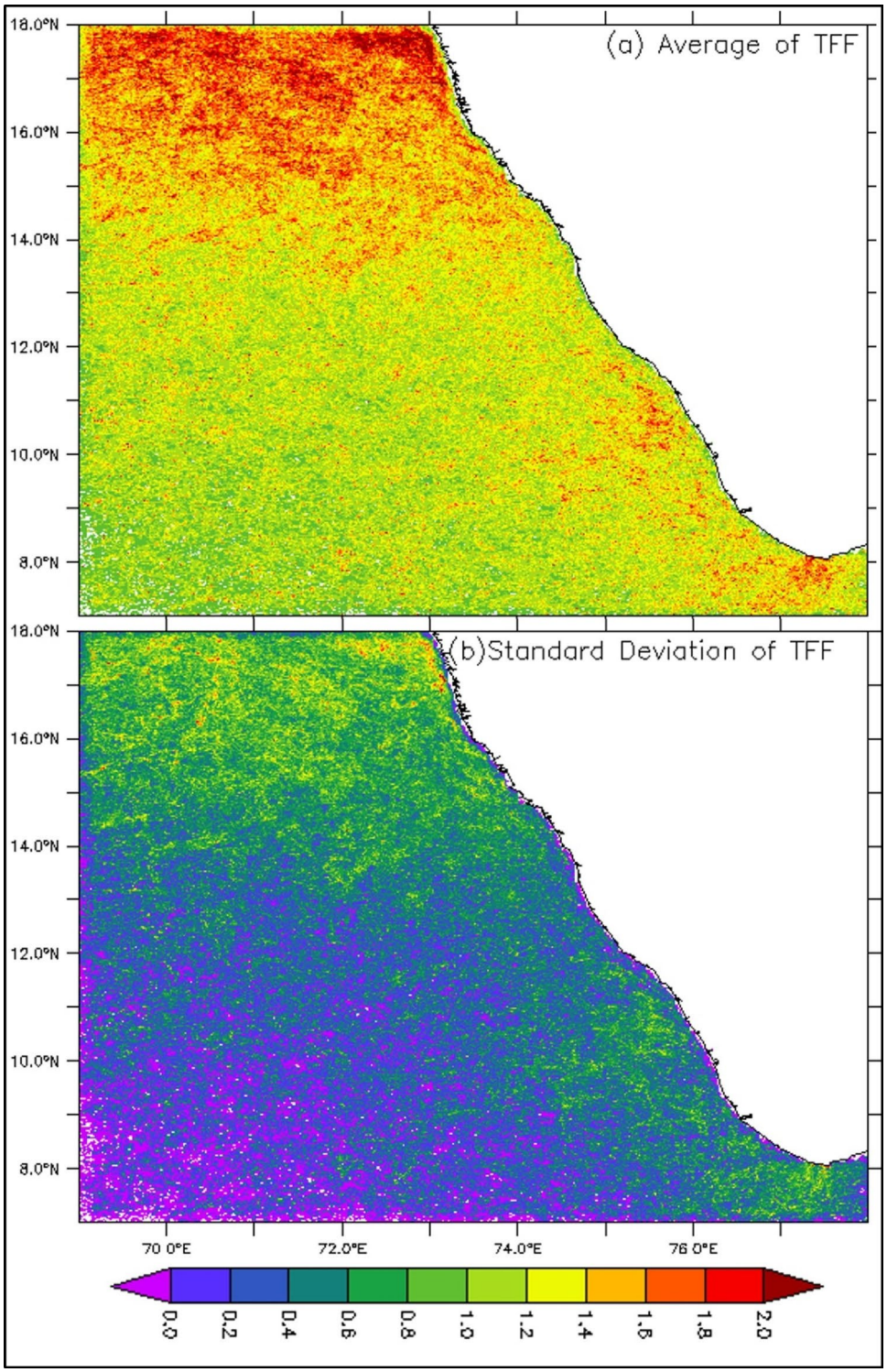


Fig. 4 Spatial distribution of **a** mean and **b** SD of TFF along the SW coast of India during January 2020 to October 2023

supportive of productivity, but nutrients dynamics regulate front variability. The mean and SD together confirm that the persistence and variability of fronts is influenced by wind induced upwelling, STF and biological factors along the SW coast of India.

Figure 5 illustrates the spatial distribution of fish catch sampling locations from the Captain Fresh dataset overlaid on the two-day lag TF map, referenced to the respective fish-catching dates. Zoomed panels provide month-wise views for clearer interpretation: (a) January, (b) February, (c) March, (d) April and (e) May. The figure shows that

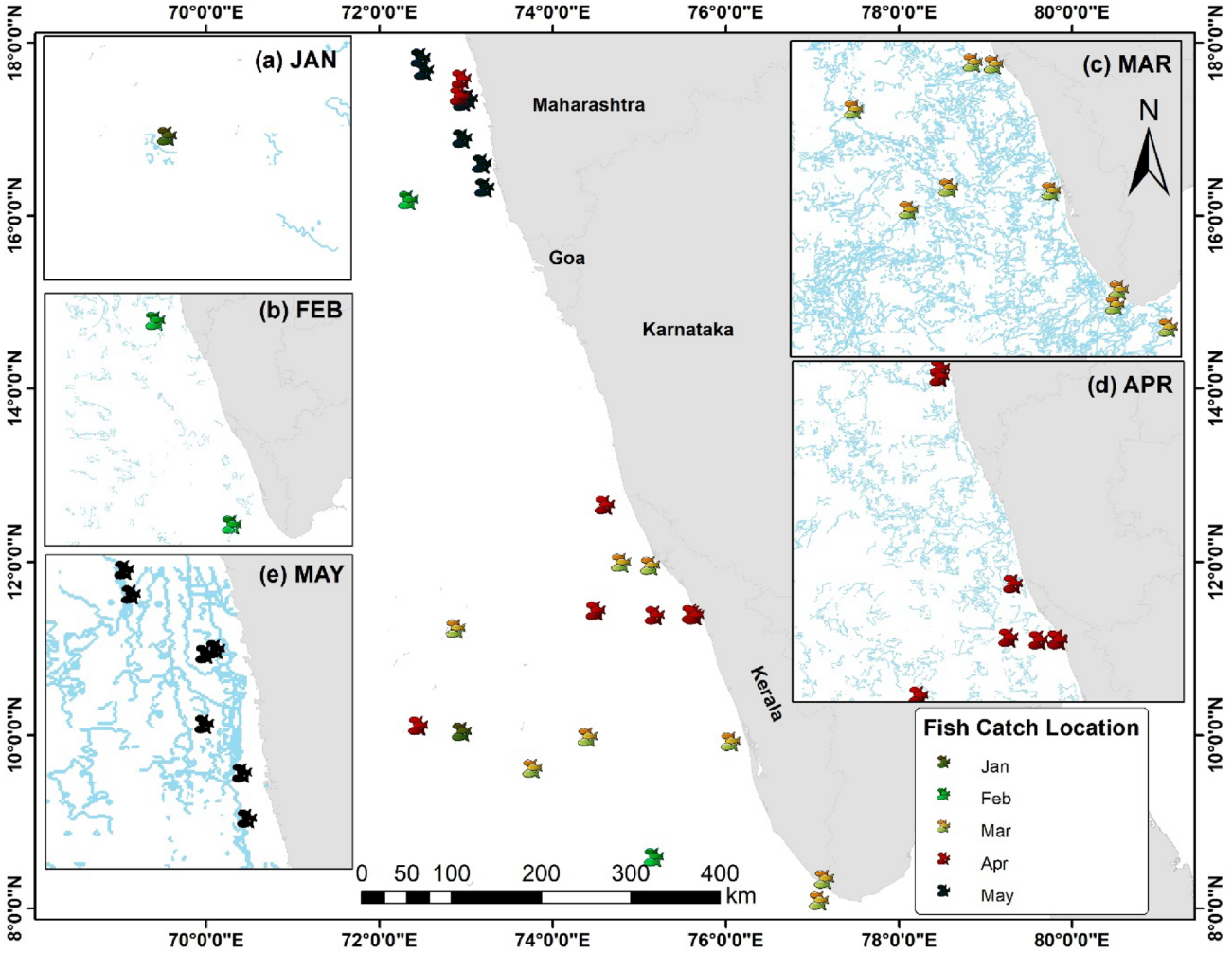


Fig. 5 Sampling locations of Captain Fresh fish catch data (26 sampling points) overlaid on the two-day lag TF map, referenced to the respective fish-catching dates. The zoomed panels illustrate the month-wise distribution of fish catch locations for improved interpretation: **a** January, **b** February, **c** March, **d** April and **e** May

higher TFD values were generally observed two days lag to the recorded fish catch events. Furthermore, the correlation of fish catch, TFD with bio-physical environmental parameters are discussed in the following section of the manuscript.

Figure 6 shows the lag/lead relationships between TFD, fish catch, chlorophyll concentration (Chl), sea-level anomaly (SLA) and geostrophic current (GC) over −6 to +6 days. The temporal relationship between TFD and fish catch showed significant variability, with the maximum correlation ($r \approx 0.40$) at −2 days (Fig. 6a), indicating that the strongest association occurred when TF preceded the fish-catch observation by about two days. The correlation then decreased to near zero lag and became weakly negative ($r \approx -0.14$), before increasing again. The better correlation at −2 days might mean that TF occurrence is a signal for favorable oceanographic conditions linked to later fish availability.

The relationship between Chl and TFD was always positive during the study period, with correlation coefficients varying approximately from 0.25 to 0.43 (Fig. 6b). The maximum correlation ($r \approx 0.43$) was found at +1 day, indicating a close temporal association between the frontal occurrence and chlorophyll variability. The answer may be related to frontal processes like water mass interaction, vertical exchange and horizontal convergence which may influence nutrient redistribution and phytoplankton concentration. But the correlation is relatively high after the front. But alone it does not prove a direct causal relation between TFD and chlorophyll enhancement.

SLA showed a different temporal pattern (Fig. 6c). For negative correlations before the frontal event, values ranged between about $r = -0.20$ at −6 days to −0.18 at −1 day and then shifted towards a positive correlation after the TFD event, peaking around $r = 0.12$ at +2 days and $r = 0.21$ at +6 days. This indicates that frontal occurrence is related to an

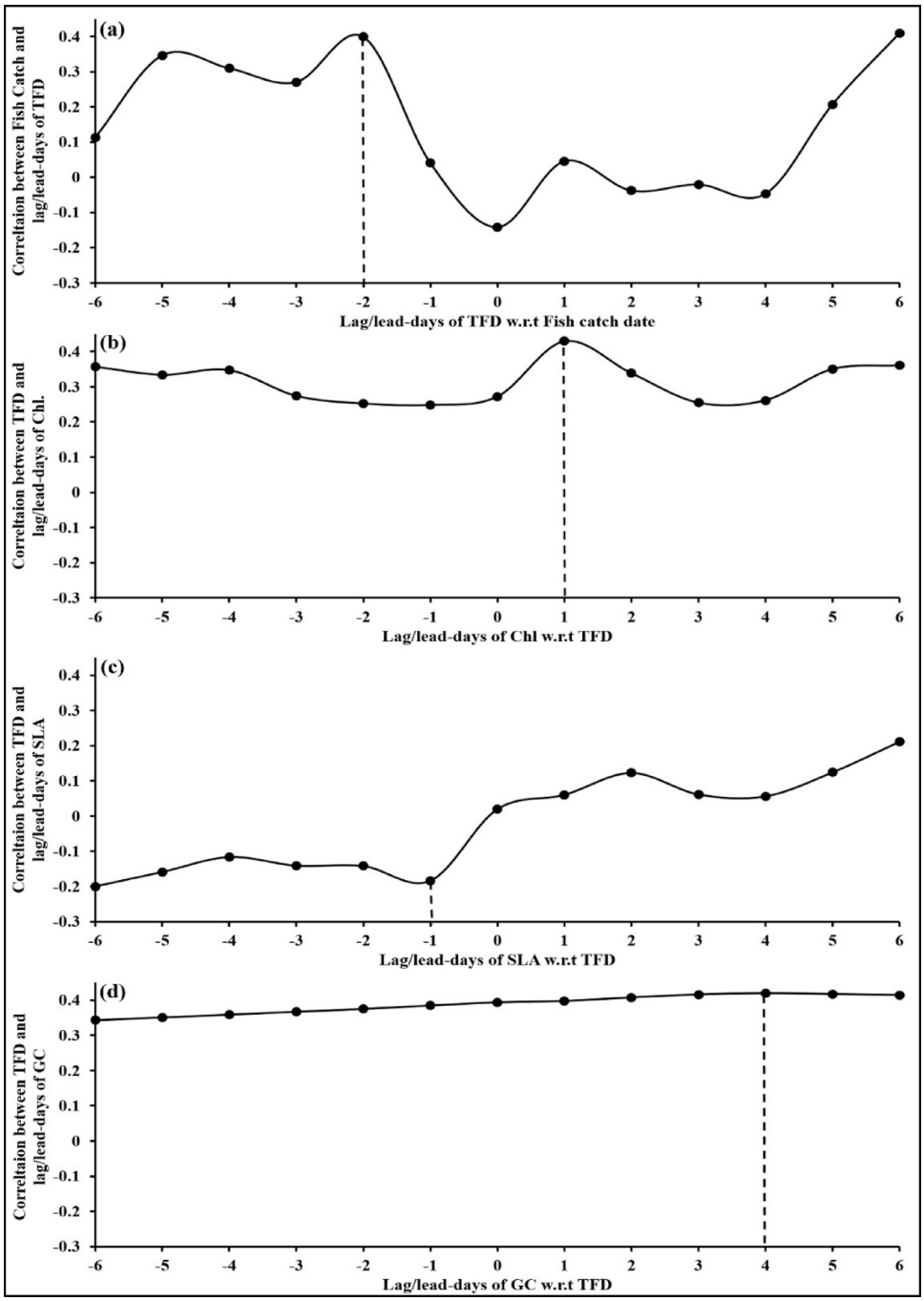


Fig. 6 showing the variability of lag/lead relationship between **a** TFD w.r.t day of fish catch, **b** concentration of chlorophyll (Chl) w.r.t days of TF **c** Sea level anomaly w.r.t days of TF and **d** Geostrophic current w.r.t days of TF

evolving sea-level and mesoscale circulation environment. Similarly, GC showed a consistently positive relationship with TFD (Fig. 6d) that increased gradually from about $r=0.34$ at −6 days to $r=0.42$ at +4 days and then remained almost stable. This suggests that TF are closely related with the prevailing geostrophic circulation, which can influence the transport and aggregation of plankton and fish prey.

Hence, the results of figure-6 observed relationships suggest that there occurs a physical-biological link between frontal structures and fish availability. The TFD development is related to changes in SLA and geostrophic currents followed by a close connection to the chlorophyll and finally fish catch. The approximately two-day lag time of fish catch on TFD could be related to the short response time of fish to a favourable area with enhanced food availability. Therefore, the TFD could be used as an indicator of an oceanic region providing a suitable habitat for fish rather than being a direct causal factor for fish catch. However, all the above statements are possible theoretical explanations for the observed correlations for the period of this study.

Figure 7 shows the scatter plots of TFD and the environmental variables detected at their optimum statistically significant lag/lead periods. There was a significant positive relationship between TFD and one-day lead chlorophyll concentration (Fig. 7a) with Kendall's $\tau = 0.35$ ($p < 0.05$) and a positive regression Sen's slope of 7.13. An increasing trend suggested that higher TFD was related to higher chlorophyll concentration about one day after the frontal condition, confirming the potential role of TF to promote or concentrate the phytoplankton by frontal mixing, water-mass interaction, and nutrients redistribution.

In contrast, TFD tended to have a weak negative relationship with the one-day lag of SLA (Fig. 7b; Kendall's $\tau = -0.127$($p < 0.05$); slope$= -0.79$). Thus, positive trends in TFD were generally related to small decreases in SLA about 1 day before the occurrence of a frontal condition. It should be noted that the magnitude of the relationship was weak, indicating that SLA is likely a subordinate physical descriptor of the evolving frontal environment rather than an important control on TFD.

A significant positive correlation was also found between TFD and the four-day lead geostrophic current (Fig. 7c), with Kendall's $\tau = 0.285$ ($p < 0.05$), and a regression slope of 2.05. The positive relationship indicates that stronger geostrophic current were associated with higher TFD approximately four days after the corresponding current condition.

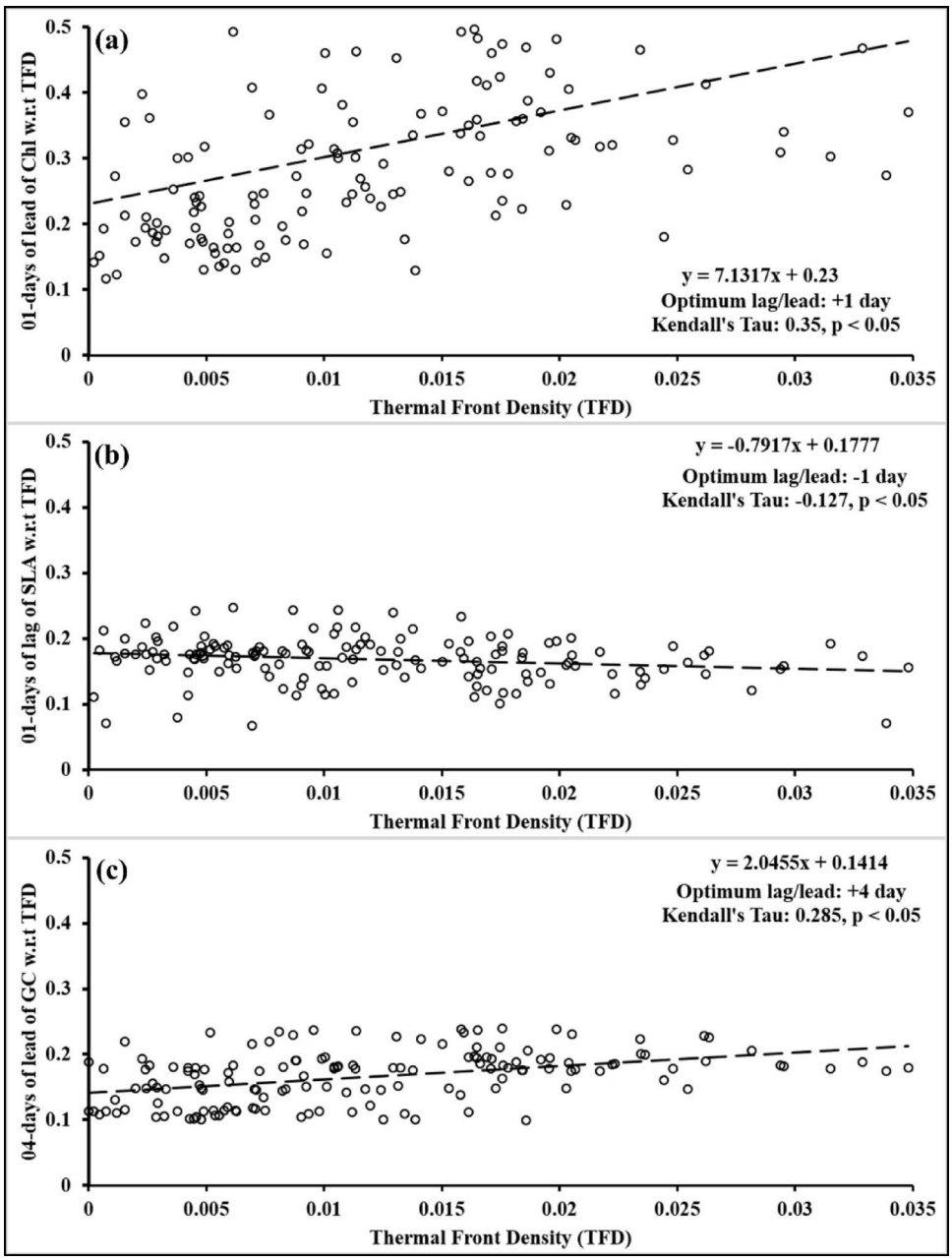


Fig. 7 showing the scattered plot of TFD at optimum days with p value less than 0.05 verses **a** one-day lead of Chlorophyll **b** one-days lag of sea level anomaly and **c** four-day lead of geostrophic current

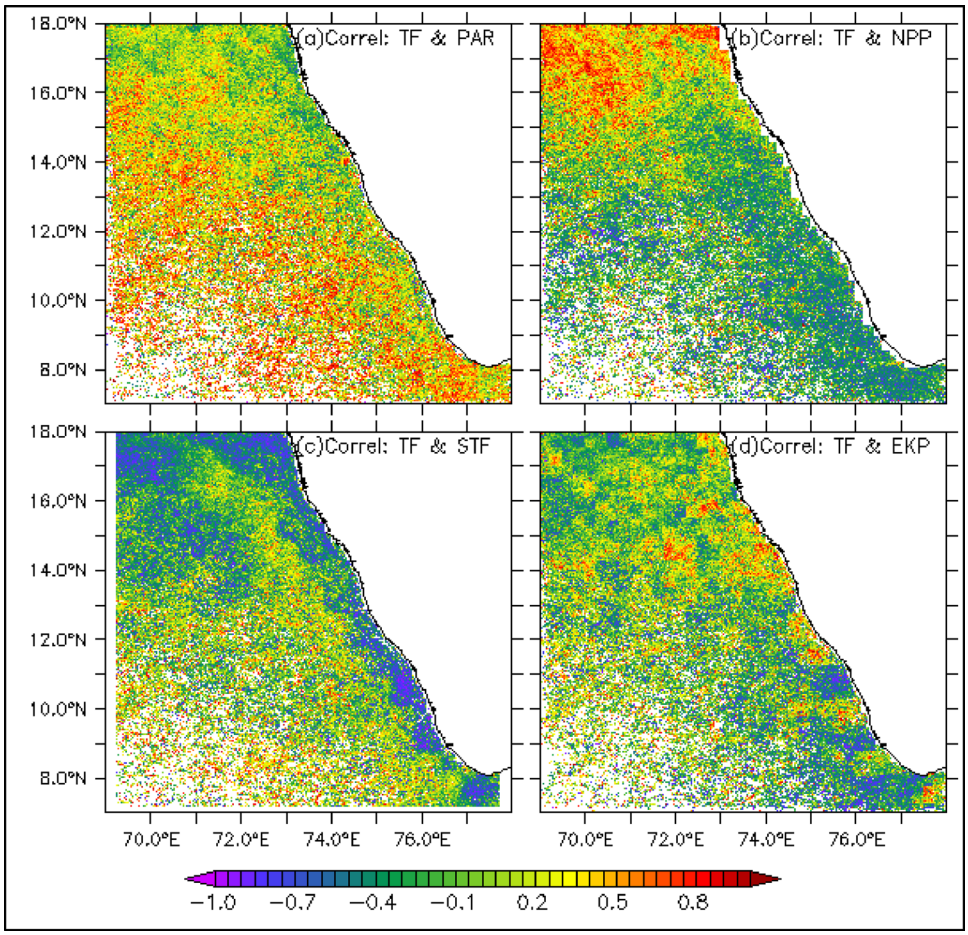


Fig. 8 Spatial distribution of Pearson's correlation coefficients between TF and key biophysical variables along the SW coast of India during study period. Panels show correlations of TF with **a** Photosynthetically Active Radiation (PAR), **b** Net Primary Productivity (NPP), **c** Stratification (STF) and **d** Ekman pumping (EKP)

This relationship suggests that the development and persistence of TF are closely related to the surrounding mesoscale circulation that can impact on the water-mass transport, frontal convergence and the aggregation or redistribution of biological material.

Overall, Fig. 7 offers statistical evidence supporting the temporal relationships established in Fig. 6. The statistically significant relationships between the TFD-Chl at +1 day, TFD-SLA at −1 day, and TFD-GC at +4 days suggest that the TFD variability is related to a series of changes in the biophysical state of the ocean. This relationship supports the interpretation that a TFD may act as an indicator of a dynamically active oceanographic environment probability of favourable for enhanced biological productivity and fish availability.

The Fig. 8 shows spatial distribution of Pearson's correlation coefficients between TF and key biophysical variables along the SW coast of India during study period. Physical forcing mechanisms like EKP and STF effect nutrient delivery and water column stability. Moderate STF can maintain phytoplankton in the euphotic layer, thereby increasing biomass production, while strong STF inhibits vertical nutrient flux (Behrenfeld et al., 2006). Therefore, weaker STF (Fig. 8c) resulted in the highly TF with high NPP (Fig. 8b) at the study area. Additionally, some regional coastal area of SW coast of India indicating the high TF with productivity zone due to upwelling zone (Fig. 8d).

The temporal difference between the peak chlorophyll-TFD correlation and the peak fish catch-TFD correlation again emphasizes trophic transfer time. Phytoplankton blooms take time to develop after nutrient enrichment, but zooplankton grazing and fish accumulation take longer. Pelagic fish have been shown to follow prey distribution and hydrographic characteristics, sometimes responding to mesoscale features like fronts and eddies (Olson et al., 1994). The two-day delay in this study is likely the time required for ecological adjustment of prey concentration and predator migration. From a fisheries point of view, these findings demonstrate the predictive capability of TFD monitoring. Real-time identification of strong frontal activity can offer early warning of high ch-a and subsequent fish accumulation within a 2–3 day time frame.

Therefore, based on observed lag/lead relationships confirm that fish availability is a consequence of trophic amplification initiated by frontal processes. Integrating satellite derived TFD with ch-a and wind-driven indices can

improve fisheries forecasting and ecosystem-based management over the study area.

In Fig. 8a, the correlation between TF and PAR is mainly positive in most offshore areas, especially south of ~ 14°N. This implies that greater frontal gradients are linked to greater surface light availability (Madhupratap et al., 1996; Vinayachandran et al., 2021). In open ocean areas, where turbidity is lower, greater PAR is likely to favour phytoplankton production in frontal convergence zones. Yet, the correlation is weaker or irregular near the coast, suggesting that light availability does not completely regulate frontal productivity. Coastal areas are more regulated by vertical mixing and nutrient inputs than surface irradiance.

In the Fig. 8b, the TF-NPP correlation reveals that the northern offshore area has a positive correlation, while the southern and nearshore areas have a weaker or negative correlation. The positive correlation in the northern area suggests that TF are responsible for biological productivity due to the aggregation of nutrients (Cayula & Cornillon, 1990). TF can trap phytoplankton biomass and act as productivity hotspots. On the other hand, the negative correlation in the southern area suggests that the intensity of TF may not be related to the aggregation of nutrients.

In the Fig. 8c illustrates the spatial pattern of the STF of the maps is the predominantly negative correlation between TF and STF, especially in the northern and central regions. This suggests that high STF is associated with low thermal frontal activity. Physically, high STF inhibits vertical mixing, reducing the entrainment of nutrients from the lower layers and the vertical density gradients that drive the dynamic sharpening of the front. On the other hand, low STF (or high mixing) is suggested to be beneficial for frontal enhancement, especially within the coastal region where the blue (negative) anomalies are strongest.

The correlation pattern Fig. 8d illustrates the TF-EKP relationship's spatial heterogeneity, with positive correlation offshore and mixed signals nearshore. Positive correlation indicates that wind-induced upwelling (positive EKP) enhances frontal gradients through the supply of nutrients and increased temperature contrasts (Sea, 2020; & Xie, 2004). Areas of negative correlation could indicate downwelling-favourable wind stress curl, which inhibits vertical nutrient transport and reduces frontal productivity. The patchy appearance of this pattern indicates that wind forcing is intermittent.

The findings show that the TF in the SW coast of India are dominantly influenced by vertical processes rather than light availability alone. The spatial correlation patterns show that TF are integrative indicators of upper-ocean physical-biological coupling. The PAR supports productivity and the strongest ecological response (positive TF-NPP correlation) is consistent with regions of moderate mixing and wind-driven upwelling. The negative TF-STF relationship highlights that too much STF inhibits frontal enhancement mechanisms.

The spatial coherence between TF, NPP and EKP in the northern offshore region indicates a dynamically active region where wind-induced processes increase nutrient delivery, favouring phytoplankton development and biomass aggregation. Such regions are potential candidates for PFZ due to the increased efficiency of trophic transfer. Variability in these regions is mainly controlled by wind-induced vertical exchange and intensity of STF.

Conclusion

This study reveals that the thermal front activity on the SW coast of India is highly variable both in space and time. Regional variability is evident which appears to be associated with the regional hydrography and physical oceanography. The relation between TF and biological productivity and their spatial correspondence with NPP suggests that they may contribute to enhanced productivity in these frontal areas by mechanisms such as nutrient redistribution, mixing and retention.

The lead-lag analysis identified a coherent short-term relationship among frontal dynamics, oceanographic conditions, productivity, and fish occurrence. The analysis revealed that chlorophyll-a was most closely related to TFD with a lead of approximately 1 day, whereas the strongest relationship between TFD and fish catch was observed with a lag of about 2 days. The similar relationships between TFD and sea level anomaly, and between TFD and geostrophic current, suggest that frontal development occurs within a dynamically evolving hydrographic and circulation environment. Nonetheless, the apparent lack of explanatory power in the TFD-fish catch relationship implies that TFDs alone cannot fully explain fish catch variability, reflecting the combined influences of prey fields, species-specific responses, circulation, and fishing effort.

Overall, satellite retrieved TF can be used as a useful ancillary indicator of potentially productive frontal habitats as well as short term fishing-habitat suitability along the SW coast of India. Incorporating TF together with chlorophyll-a, NPP, geostrophic currents, sea-level anomaly and fisheries observations would improve characterization of PFZ and contribute to more comprehensive ecosystem-based fisheries applications. Further validation with spatially representative fisheries data, standardized CPUE as well as additional biological and oceanographic observations is required to ascertain robustness and operational utility of these relationships.

However, establishing end-to-end linkages would require further studies that would provide additional measurements of biogeochemical and ecological variables such as nutrients, primary production, zooplankton, fisheries resources, and fishing effort, which is beyond this study's scope. This limitation can be overcome in future studies by integrating the present observations to identify the underlying processes or mechanisms.

Acknowledgements The authors are thankful to Director, INCOIS for facility and motivation. Thanks to Dukes, Nicholas School of the Environment and MGET development team for making MGET tool available on their website. Thanks to NOAA for avaiability of Chlorophyll, SST, NPP and PAR in public domain. Authours also like to thanks GODAS for avalability of ocean column temparature and sality in public domain. Thanks to the FERRET development team for making available FERRET available online. The authors also express thanks to Captain Fresh for collecting and sharing geotagged fish catch data from the Indian Ocean region. This is INCOIS publication contribution number 737.

Author contributions All authors substantially contributed to completing this research article. The individual authors` contributions are that Mr. Harisha Rathod has prepared the original draft of the article and incorporated all the corrections suggested by co-authors. Mr. Harisha Rathod and Dr PC Mohanty, who set up the conception of the framework of the study, data analysis and interpretation of the data. Ms. J. Nithya and J. Karthi are contributed to carry out the analysis and interpretation of results. Dr Dhanya M Lal, Mr Alakes Samanta and Dr Sanjiba Kumar Baliarsingh contribute data curation, writing-review & editing. Dr Sudheer Josheph and Dr Balakrishnan Nair T M contribute to the guidance, supervision, advice and revision of the essential intellectual content of the manuscript. All the authors contributed to the final approval of the version to be submitted.

Funding The authors declare that no funds, grants, or other support were received during the preparation of this manuscript.

Data Availability All the data sources that are well-detailed in the methodology section will be available upon request.

Declarations

Conflict of interest The authors declare that the research was conducted in the absence of any commercial or financial relationships that could be construed as a potential conflict of interest.

References

Behrenfeld, M. J., O'Malley, R. T., Siegel, D. A., McClain, C. R., Sarmiento, J. L., Feldman, G. C., Milligan, A. J., Falkowski, P. G., Letelier, R. M., & Boss, E. S. (2006). Climate-driven trends in contemporary ocean productivity. *Nature*, *444*(7120), 752–755.

Belkin, I. M., Cornillon, P. C., & Sherman, K. (2009). Fronts in large marine ecosystems. *Progress in Oceanography*, *81*(1–4), 223–236. https://doi.org/10.1016/j.pocean.2009.04.015

Bost, C. A., Cotté, C., Bailleul, F., Cherel, Y., Charrassin, J. B., Guinet, C., Ainley, D. G., & Weimerskirch, H. (2009). The importance of oceanographic fronts to marine birds and mammals of the southern oceans. *Journal of Marine systems*, *78*(3), 363–376.

Bruce, J. G., Johnson, D. R., & Kindle, J. C. (1994). Evidence for eddy formation in the eastern Arabian Sea during the northeast monsoon. *Journal of Geophysical Research: Oceans, 99*(C4), 7651–7664.

Castillo, J., Barbieri, M. A., & Gonzalez, A. (1996). Relationships between sea surface temperature, salinity and pelagic fish distribution off northern Chile. *ICESJ Mar Sci*, *53*, 139–146. https://doi.org/10.1006/jmsc.1996.0014

Cayula, J. F. P., & Cornillon, P. C. (1990, November). Edge detection applied to SST fields. In Digital image processing and visual communications technologies in the earth and atmospheric sciences (Vol. 1301, pp. 13–24).

Cayula, J. F., & Cornillon, P. (1992). Edge detection algorithm for SST images. *Journal of atmospheric and oceanic technology*, *9*(1), 67–80.

Chakraborty, K., Maity, S., Lotliker, A. A., Samanta, A., Ghosh, J., Masuluri, N. K., Swetha, N., & Bright, R. P. (2019). Modelling of marine ecosystem in regional scale for short term prediction of satellite-aided operational fishery advisories. *Journal of Operational Oceanography*, *12*(sup2), S157–S175.

CMFRI. (2024). *Annual Report 2023* (p. 286). Central Marine Fisheries Research Institute.

Cox, S. L., Miller, P. I., Embling, C. B., Scales, K. L., Bicknell, A. W., Hosegood, P. J., Morgan, G., Ingram, S. N., & Votier, S. C. (2016). Seabird diving behaviour reveals the functional significance of shelf-sea fronts as foraging hotspots. *Royal Society Open Science, 3*(9), Article 160317.

Das, S., Madhu, V. R., Sreejith, P. T., Jethva, J. K., & Meenakumari, B. (2010). Validation of potential fishing zones along saurashtra coast, Gujarat. In: Proceedings of the National Seminar on Conservation and Sustainability of Coastal Living Resources of India, Cochin, 1–3 December2009, pp.138–144. http://hdl.handle.net/123456789/1578

Deshpande, S. P., Radhakrishnan, K. V., & Bhat, U. G. (2011). Direct and indirect validation of potential fishing zone advisory off the coast of Uttara Kannada, Karnataka. *Journal of the Indian Society of Remote Sensing, 39*(4), 547–554.

Dwivedi, R. M., Solanki, H. U., Nayak, S. R., Gulati, D., & Somvanshi, V. S. (2005). Exploration of fishery resources through integration of ocean colour with sea surface temperature: Indian experience. *Indian J Mar Sci*, *34*(4), 430–440.

Ebango Ngando, N., Song, L., Cui, H., & Xu, S. (2020). Relationship between the spatiotemporal distribution of dominant small pelagic fishes and environmental factors in Mauritanian waters. *Journal of Ocean University of China*, *19*(2), 393–408.

Food and Agriculture Organization of the United Nations. (2020). *The state of world fisheries and aquaculture 2020: Sustainability in action*. FAO. https://doi.org/10.4060/ca9229en

Food and Agriculture Organization of the United Nations. (2024). *The state of world fisheries and aquaculture 2024: Blue transformation in action*. FAO. https://doi.org/10.4060/ccf508en

Gill, A. E. (1982). *Atmosphere-Ocean Dynamics*. University of Cambridge.

Habeebrehman, H., Prabhakaran, M. P., Jacob, J., Sabu, P., Jayalakshmi, K. J., Achuthankutty, C. T., & Revichandran, C. (2008). Variability in biological responses influenced by upwelling events in the Eastern Arabian Sea. *Journal of Marine Systems*, *74*(1–2), 545–560.

Jishad, M., & Agarwal, N. (2022). Thermal front detection using satellite-derived sea surface temperature in the northern indian ocean: Evaluation of gradient-based and histogram-based methods. *Journal of the Indian Society of Remote Sensing*, *50*(7), 1291–1299.

Lal, D. M., Samanta, H., Joseph, A., Kumar, S., Baliarsingh, S. S., S. K., & Nair, T. B. (2025). Validation and assessment of Potential Fishing Zone (PFZ) dynamics along the southwest coast of India

through environmental proxies and trophic guild analysis. *Environmental Impact Assessment Review*, *114*, 107953.

Madhupratap, M., Gopalakrishnan, T. C., Haridas, P., & Nair, K. K. C. (2001). Mesozooplankton biomass, composition and distribution in the Arabian Sea during the fall intermonsoon: Implications of oxygen gradients. *Deep Sea Research Part II: Topical Studies in Oceanography*, *48*(6–7), 1345–1368.

Madhupratap, M., Kumar, S. P., Bhattathiri, P. M. A., Kumar, M. D., Raghukumar, S., Nair, K. K. C., & Ramaiah, N. (1996). Mechanism of the biological response to winter cooling in the northeastern Arabian Sea. *Nature*, *384*(6609), 549–552.

Miller, P. I., Scales, K. L., Ingram, S. N., Southall, E. J., & Sims, D. W. (2015). Basking sharks and oceanographic fronts: Quantifying associations in the north-east Atlantic. *Functional Ecology, 29*(8), 1099–1109.

Mohanty, P. C., Mahendra, R. S., Nayak, R. K., Kumar, N., Kumar, T. S., & Dwivedi, R. M. (2017). Persistence of productive surface thermal fronts in the northeast Arabian Sea. *Regional Studies in Marine Science*, *16*, 216–224. https://doi.org/10.1016/j.rsma.2017.09.010

Mugo, R. M., Saitoh, S. I., Takahashi, F., Nihira, A., & Kuroyama, T. (2014). Evaluating the role of fronts in habitat overlaps between cold and warm water species in the western North Pacific: A proof of concept. *Deep Sea Research Part II: Topical Studies in Oceanography, 107*, 29–39.

Nammalwar, P., Satheesh, S., & Ramesh, R. (2013). Applications of remote sensing in the validations of potential fishing zones (PFZ) along the coast of North Tamil Nadu, India. *Indian J Geo-Marine Sci*, *42*(3), 283–292.

Nayak, S. R., Solanki, H. U., & Dwivedi, R. M. (2003). Utilization of IRS P4 ocean colour data for potential fishing zone–a cost benefit analysis. *Indian J Mar Sci*, *32*(3), 244–248.

Nieblas, A. E., Demarcq, H., Drushka, K., Sloyan, B., & Bonhommeau, S. (2014). Front variability and surface ocean features of the presumed southern bluefin tuna spawning grounds in the tropical southeast Indian Ocean. *Deep Sea Research Part II: Topical Studies in Oceanography*, *107*, 64–76.

Olson, D. B., Hitchcock, G. L., Mariano, A. J., Ashjian, C. J., Peng, G., Nero, R. W., & Podestá, G. P. (1994). Life on the edge: Marine life and fronts. *Oceanography, 7*(2), 52–60.

Pauly, D., & Palomares, M. L. (2005). Fishing down marine food web: It is far more pervasive than we thought. *Bulletin Of Marine Science*, *76*(2), 197–212.

Pillai, V. N., & Nair, P. G. (2010). Potential fishing zone (PFZ) advisories-Are they beneficial to the coastal fisherfolk? A case study along Kerala coast, South India. In Biological Forum (Vol. 2, No. 2, pp. 46–55).

Polovina, J. J., Howell, E., Kobayashi, D. R., & Seki, M. P. (2001). The transition zone chlorophyll front, a dynamic global feature defining migration and forage habitat for marine resources. *Progress in oceanography*, *49*(1–4), 469–483. https://doi.org/10.1016/S0079-6611(01)00036-2

Reese, D. C., O'Malley, R. T., Brodeur, R. D., & Churnside, J. H. (2011). Epipelagic fish distributions in relation to thermal fronts in a coastal upwelling system using high resolution remote-sensing techniques. *ICES Journal of Marine Science*, *68*(9), 18651874.

Sarkar, K., Aparna, S. G., Dora, S., & Shankar, D. (2019). Seasonal variability of sea-surface temperature fronts associated with large marine ecosystems in the north Indian Ocean. *Journal of Earth System Science*, *128*(1), 20.

Sarma, V. V. S. S., Desai, D. V., Patil, J. S., Khandeparker, L., Aparna, S. G., Shankar, D., D`Souza, S., Dalabehera, H. B., Mukherjee, J., Sudharani, P., & Anil, A. C. (2018). Ecosystem response in temperature fronts in the northeastern Arabian Sea. *Progress in Oceanography*, *165*, 317–331. https://doi.org/10.1016/j.pocean.2018.02.004

Sarupria, J. S., & Bhargava, R. M. S. (1993). Seasonal primary production in different sectors of the EEZ of India.

Scales, K. L., Miller, P. I., Varo-Cruz, N., Hodgson, D. J., Hawkes, L. A., & Godley, B. J. (2015). Oceanic loggerhead turtles Caretta caretta associate with thermal fronts: Evidence from the Canary Current Large Marine Ecosystem. *Marine Ecology Progress Series*, *519*, 195–207.

Schott, F. A., & McCreary, J. P., Jr. (2001). The monsoon circulation of the Indian Ocean. *Progress in Oceanography, 51*(1), 1–123.

Sea, S. C. (2020). Coastal upwelling. *Regional Oceanography Of The South China Sea*, 289.

Shankar, D., Shenoi, S. S. C., Nayak, R. K., Vinayachandran, P. N., Nampoothiri, G., Almeida, A. M., Michael, G. S., Kumar, R., Sundar, M. R., D., & Sreejith, O. P. (2005). Hydrography of the eastern Arabian Sea during summer monsoon 2002. *Journal of earth system science*, *114*(5), 459–474.

Shankar, D., Vinayachandran, P. N., & Unnikrishnan, A. S. (2002). The monsoon currents in the north Indian Ocean. *Progress in oceanography*, *52*(1), 63–120.

Shetye, S. R., Gouveia, A. D., Shenoi, S. S. C., Sundar, D., Michael, G. S., Almeida, A. M., & Santanam, K. (1990). Hydrography and circulation off the west coast of India during the southwest monsoon 1987.

Solanki, H. U., Dwivedi, R. M., & Narain, A. (1998). Satellite observations of coastal upwelling in the Northern Arabian Sea and its impact on fishery resources. In: Proceedings of the International Symposium on Information Technology in Oceanography, ITO, October, Goa, India, pp. 12–16.

Solanki, H. U., Dwivedi, R. M., & Nayak, S. R. (2001a). Synergistic analysis of SeaWiFS chlorophyll concentration and NOAA-AVHRR SST features for exploring marine living resources. *International Journal Of Remote Sensing*, *22*, 3877–3882.

Solanki, H. U., Dwivedi, R. M., Nayak, S. R., Jadeja, J. V., Thaker, D. B., Dave, H. B., & Patel, M. I. (2001b). Application of ocean colour monitor chlorophyll and AVHRR SST for fishery forecast. Preliminary validation results off Gujarat Coast, North West of India. *Ind J Marine Sci*, *30*, 132–138.

Solanki, H. U., Dwivedi, R. M., Nayak, S. R., Somvanshi, V. S., Gulati, D. K., & Pattnayak, S. K. (2003). Fishery forecast using OCM chlorophyll concentration and AVHRR SST: Validation results off Gujarat coast, India. *International Journal of Remote Sensing, 24*(18), 3691–3699.

Solanki, H. U., Mankodi, P. C., Dwivedi, R. M., & Nayak, S. R. (2008). Satellite observations of main oceanographic processes to identify ecological associations in the Northern Arabian Sea for fishery resources exploration. *Hydrobiologia*, *612*, 269–279. https://doi.org/10.1007/s10750-008-9496-8

Solanki, H. U., Mankodi, P. C., Nayak, S. R., & Somvanshi, V. S. (2005). Evaluation of remote-sensing-based potential fishing zones (PFZs) forecast methodology. *Continental Shelf Research*(18). https://doi.org/10.1016/j.csr.2005.08.025

Solanki, H. U., Prakash, P., Dwivedi, R. M., Nayak, S., Kulkarni, A., & Somvamshi, V. S. (2010). Synergistic application of oceanographic variables from multi-satellite sensors for forecasting potential fishing zones: Methodology and validation results. *International Journal of Remote Sensing, 31*(3), 775–789.

Subramanian, S., Sreekanth, G. B., Manjulekshmi, N., Narendra, Pratap, Singh,, J., Kolwalkar,, T., Patil, & Fernandes, P. M. (2014). *Manual on the Use of Potential Fishing Zone (PFZ) Forecast. Technical Bulletin No. 40*. ICAR Research Complex for Goa (Indian Council of Agricultural Research).

Swapna, M., Raju, R., Nayak, R. K., Mohanty, P. C., SeshaSai, M. V. R., & Kumar, R. (2023). Spatiotemporal characteristics of thermal fronts in relation to potential fishing zones in the continental shelf sea around India. *Journal of the Indian Society of Remote Sensing*, *51*(2), 335–348.

Tseng, C. T., Sun, C. L., Belkin, I. M., Yeh, S. Z., Kuo, C. L., & Liu, D. C. (2014). *Sea surface temperature fronts affect distribution of Pacific saury (Cololabis saira) in the Northwestern Pacific Ocean* (Vol. 107, pp. 15–21). Topical Studies in Oceanography.

Vinayachandran, P. N. M., Masumoto, Y., Roberts, M. J., Huggett, J. A., Halo, I., Chatterjee, A., Amol, P., Gupta, G. V. M., Singh, A., Mukherjee, A., Prakash, S., Beckley, L. E., Raes, E. J., & Hood, R. (2021). Reviews and syntheses: Physical and biogeochemical processes associated with upwelling in the Indian Ocean. *Biogeosciences, 18*(22), 5967–6029.

Wyrtki, K. L. A. U. S. (1973). Physical oceanography of the Indian Ocean. *The biology of the Indian Ocean* (pp. 18–36). Springer Berlin Heidelberg.

Xie, S. P. (2004). Satellite observations of cool ocean–atmosphere interaction. *Bulletin of the American Meteorological Society, 85*(2), 195–208.

Yang, K., Meyer, A., Strutton, P. G., & Fischer, A. M. (2023). Global trends of fronts and chlorophyll in a warming ocean. *Communications Earth & Environment*, *4*(1), 489.

Publisher's Note Springer Nature remains neutral with regard to jurisdictional claims in published maps and institutional affiliations.

Springer Nature or its licensor (e.g. a society or other partner) holds exclusive rights to this article under a publishing agreement with the author(s) or other rightsholder(s); author self-archiving of the accepted manuscript version of this article is solely governed by the terms of such publishing agreement and applicable law.